Dalton Transactions

COMMUNICATION

View Article Online
View Journal

Check for updates

Cite this: DOI: 10.1039/c8dt02933d

Received 18th July 2018,
Accepted 14th August 2018

DOI: 10.1039/c8dt02933d

rsc.li/dalton

Bisphosphine phenol and phenolate complexes of Mn(I): manganese(I) catalyzed Tishchenko reaction†

Karthika J. Kadassery,[a] Samantha N. MacMillan[b] and David C. Lacy*[a]

We synthesized new organomanganese complexes using the phenolic "pincer" type ligand H-POP. The coordination chemistry of H-POP with Mn(I) was explored, revealing a wide range of binding motifs. Finally, we found that complex 1 catalyzes the formation of benzyl benzoate from benzaldehyde in a Tishchenko reaction.

Ruthenium pincer compounds are excellent catalysts in a variety of applications but suffer from the fact that ruthenium is an expensive metal.[1] In principle, analogous chemistry should be accessible with low-spin Mn(I) d^6 ions because of its similarity in ionic radii to d^6 Ru(II) ions.[2] Indeed, recent advances with manganese catalysts with pincer ligands attests to this possibility of replacing Ru with non-precious Mn and warrants further exploration of the coordination chemistry of Mn(I) on new platforms.[3–7] To this end, we have explored the coordination chemistry and catalytic activity of the first Mn(I) complexes with bisphosphine phenol and phenolate ligands and report our findings herein. While POP "pincer" ligands have been extensively studied,[8] phenolic based POP "pincer" phosphine ligands have not been explored with the exception of d^8 ions such as Rh(I), Ni(II), and Pd(II).[9–11] In part, the lack of phenolic ligands in organometallic catalysis is due to the fact that electron rich metal ions often oxidatively add across the phenolic C–O bond, forming a traditional PCP pincer complex.[12] This C–O bond cleavage reaction unfortunately hinders coordination studies of organometallic phenolic complexes. Conveniently, Mn(I) ions are not prone to undergo oxidative addition and therefore enabled our investigation of the coordination chemistry of phenolic platforms and possibly discover new applications in catalysis.

Our entry into the phenolic Mn(I)POP complexes utilized a known synthetic route to prepare the cresol variant of Yamane's bis(diphenylphosphine)phenol ligand.[9,13] The synthesis is a two step process, the first of which involves dialkylation of *p*-cresol with formaldehyde and amination with aqueous dimethylamine forming 2,6-bis[(dimethylamino)methyl]-4-methylphenol (**H-NON**) in 57% yield (Scheme 1). The diamine is heated in neat diphenylphosphine wherein a quinone methide intermediate,[14] generated by liberation of dimethylamine, is attacked by the phosphine. Excess Ph_2PH is important in the final step to ensure that the reaction continues in solvent, which is easily removed afterwards by washing with copious amounts of petroleum ether and recovered for future reactions. The oxygen sensitive **H-POP** product is a sticky, colorless transparent gel.

With ligand in hand, we attempted various methods of installing Mn(I) ions to **H-POP**. In a previous report, we showed that treatment of $Mn_2(CO)_{10}$ with 6 eq. Me_3NO in rigorously dry toluene afforded the tetranuclear complex $[\{Mn(CO)_3\}_2(\mu\text{-}ONMe_3)]\{(\mu\text{-}CO_3)[Mn(NMe_3)(CO)_3]\}_2$ (**Mn₄**).[15] Complex **Mn₄** contains two basic carbonato ligands and two trimethylamine ligands that participate in deprotonating water and form the tetrameric complex $[Mn(CO)_3(\mu_3\text{-}OH)]_4$. In an analogous reaction, replacing water with **H-POP** and treating it with *in situ* prepared **Mn₄** afforded **POP**$Mn(CO)_3$ (**1**) in 39% crystalline yield. Crystallization of **1** at −35 °C provided suitable crystals for XRD and revealed meridional $Mn(CO)_3$ coordination (Fig. 1). Recrystallization of **1** at room temperature however afforded pure dimeric complex (**1₂**) with each of the two Mn(I) centers binding to one phosphine arm in both ligands (Fig. 2). The dimeric species **1₂** is sparingly soluble in organic solvents and appears to be a sink as heating or irradiating **1** causes its irreversible conversion to the dimer.

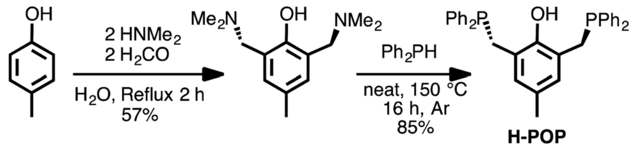

Scheme 1 Synthesis of H-POP.

---

[a] *Department of Chemistry, University at Buffalo, State University of New York, Buffalo, New York 14260, USA. E-mail: dclacy@buffalo.edu*

[b] *Department of Chemistry and Chemical Biology, Cornell University, Ithaca, New York 14853, USA*

† Electronic supplementary information (ESI) available. CCDC 1847482–1847485. For ESI and crystallographic data in CIF or other electronic format see DOI: 10.1039/c8dt02933d

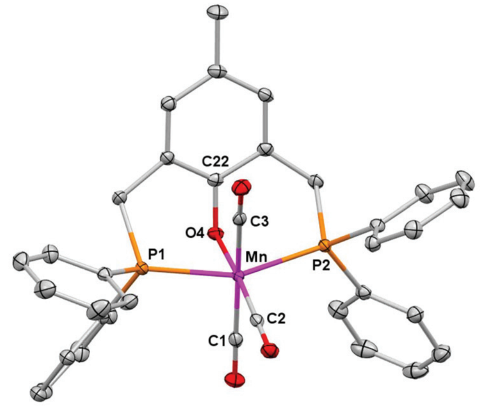

Fig. 1 Molecular structure of **1**; H-atoms and DCM solvent molecules have been removed for clarity (ellipsoids at 50% probability). Color scheme: Mn = magenta; O = red; P = orange; Br = tan; C = grey. Selected bond distances (Å) and angles (°): Mn–O4 = 2.051(2); Mn–P1 = 2.3117(6); Mn–P2 = 2.3153(6); Mn–C_{ave} = 1.83 (±0.04); C22–O4–Mn = 103.4(1); P1–Mn–P2 = 152.38(2).

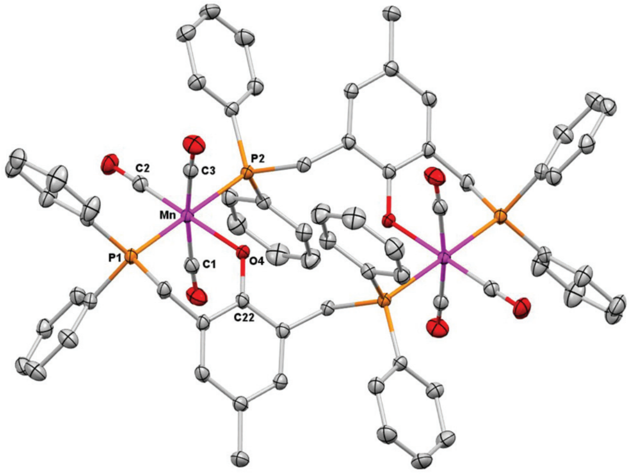

Fig. 2 Molecular structure of $\mathbf{1_2}$; H-atoms and THF solvent molecules have been removed for clarity (ellipsoids at 50% probability). Color scheme same as Fig. 1. Selected bond distances (Å) and angles (°): Mn–O4 = 2.071(2); Mn–P1 = 2.2689(6); Mn–P2 = 2.3125(6); Mn–C_{ave} = 1.83 (±0.04); C22–O4–Mn = 124.1(1); P1–Mn–P2 = 176.48(3).

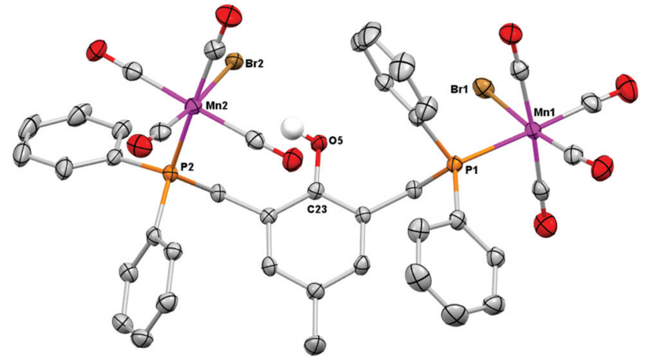

Fig. 3 Molecular structure of **2**; except for the H-atom attached to O5, H-atoms are removed for clarity (ellipsoids at 50% probability). Color scheme same as Fig. 1. Selected bond distances and angles: Mn1–Br1 = 2.519(1); Mn1–P = 2.355(1); Mn1–C_{ave} = 1.85 (±0.04); O5–Br1 = 4.536(2); O5–Br2 = 3.243(2); Mn2–Br = 2.515(1).

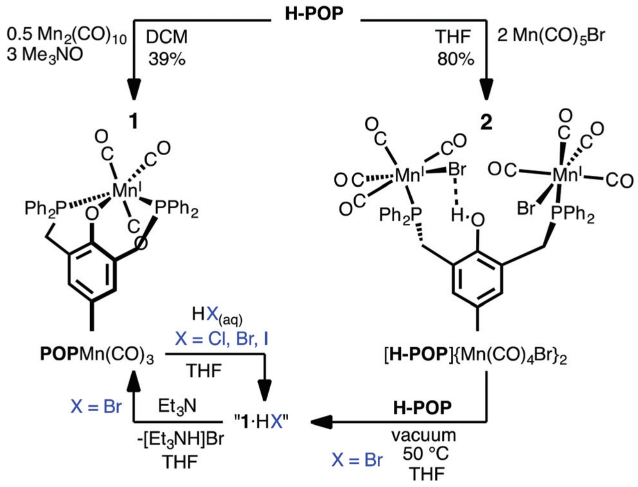

Scheme 2 Synthesis of **H-POP** Mn(I) Precursors (yields calculated for isolated crystalline material).

The synthesis of **1** through $\mathbf{Mn_4}$ is not high yielding and therefore we explored alternative synthetic routes to **1**. Treatment of **H-POP** with $Mn(CO)_5Br$ in a 1 : 1 stoichiometry in THF or DCM for 3 h results in an incomplete coordination reaction between the ligand and metal. Monitoring the reaction with ^{31}P NMR revealed three major species (Fig. S13†), one of which is free unbound ligand (^{31}P NMR −16 ppm). The other two species are partially bound ligand (free phosphine arm, ^{31}P NMR −18 ppm) and {**H-POP**}$\{Mn(CO)_4Br\}_2$ (**2**) (^{31}P NMR 40 ppm), the latter of which was characterized by X-ray crystallography (Fig. 3). Complex **2** was independently synthesized by mixing **H-POP** with $Mn(CO)_5Br$ in a 1 : 2 stoichiometry in THF at room temperature and recrystallizing from THF/hexane layering (Scheme 2) in ≥80% crystalline yield, but the reaction is essentially quantitative. The molecular structure of **2** shows that the oxygen atom of **H-POP** does not directly interact with either of the two Mn ions and that each of the Mn centers is coordinated to one of the phosphine arms of the ligand. The OH moiety is H-bonded to one of the Br ligands as indicated by a short O⋯Br distance of 3.245(2) Å. The remainder of the coordination sphere for each of the two Mn ions is occupied by four carbonyl ligands. Assuming C_s symmetry, the structure is consistent with the ^1H NMR and FTIR (solid state ATR and solution state transmission) spectrum (Fig. S10–12†), which has four CO stretches and indicates that the two Mn centers are equivalent by at least a plane of symmetry in solution.

Complex **2** reacts slowly with excess ligand at room temperature forming a new species (^{31}P NMR 55 ppm) designated **1**·HBr. When the mixture is exposed to static vacuum, several unidentified species form that disappear upon heating to

50 °C and results in the complete conversion to the same **1**·HBr species at 55 ppm (Fig. S13†). **1**·HBr is conveniently generated by mixing **H-POP** with Mn(CO)$_5$Br in a 1 : 1 stoichiometry, degassing with freeze pump thaw cycles, and heating at 50 °C for two days (Scheme 3). While no crystal structure of **1**·HBr was obtained, the CHN analysis supports the assigned empirical formula of **1**·HBr·THF and is an essentially quantitative process.

The ^{31}P NMR spectrum of **1**·HBr actually contains two peaks (Fig. S14†), one at 55.10 ppm and a major peak at 55.35 ppm that we tentatively assign to a dimer and a monomer, respectively. The major monomeric component (Scheme 3), designated [**1H**]Br, can be isolated from the mixture by washing solid **1**·HBr with toluene/Et$_2$O and collecting the remaining solids (the washings however always contain both species). The ^{1}H NMR spectrum of [**1H**]Br in DCM displays peaks similar in position to **1** and **2** but significantly more broad. The FTIR spectrum of [**1H**]Br contains three ν_{CO} in a pattern that is expected for a monomeric [**H-POP**Mn(CO)$_3$] Br formulation with meridional CO coordination (Fig. S17†). Treatment of this tentatively assigned monomer [**1H**]Br with Et$_3$N furnishes **1** and [Et$_3$NH]Br in quantitative yield. However, the mixture of the monomeric and dimeric species of **1**·HBr produces an equivalent mixture of **1** and **1$_2$** when reacted with Et$_3$N. The process is apparently reversible as a reaction between **1** in THF and HBr$_{(aq)}$ forms **1**·HBr (*vide infra*); a similar reversible ligand protonation/deprotonation was recently observed by Kirchner and coworkers.[16]

A possible structure for the second component of **1**·HBr is a dimeric molecule, [**1HBr**]$_2$, similar to **1$_2$**, with inner sphere bromido ligands and non-coordinating phenol O-atoms (Scheme 3). The –OH group on phenol might be hydrogen bonded to the coordinated Br ligand, similar to the interaction we observed in **2**. Furthermore, the structure proposed for [**1HBr**]$_2$ can easily be reconciled with the synthetic protocol for **1**·HBr from **2**. Yet another string of evidence supporting our assignment is that treatment of **1** in THF with HCl$_{(aq)}$ forms a new single species with a resonance at 57.85 ppm in the ^{31}P NMR spectrum. Similarly, treatment of **1** in THF with HI$_{(aq)}$ forms a species with a resonance at 53.92 ppm (^{31}P NMR). These shifts of about 2 ppm in the ^{31}P NMR is expected for Mn(I) carbonyl-bisphosphine complexes with different coordinated halides;[17] this serves as our primary evidence that the halide is bonded to the Mn(I) ions in [**1HX**]$_2$ (X = Cl, Br, I). The new halido species have FTIR spectra essentially identical to **1**·HBr with the exception of a shift in the ν_{OH} from 3300 cm^{-1} for X = Br to 3255 cm^{-1} for X = Cl and 3360 cm^{-1} for X = I indicating that the O–H groups of the **H-POP** ligand are H-bonded to the halide ion (Fig. S20 and S21†).

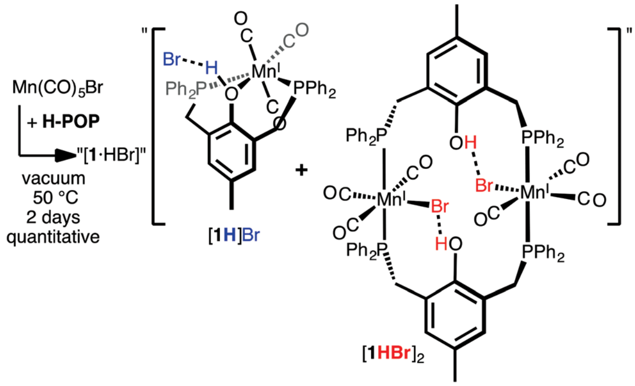

Scheme 3 Preparation and proposed speciation of **1**·HBr in THF.

Desiring to generate a 16-electron complex for catalysis, we treated **1**, **2**, and **1**·HBr with various reagents to abstract bromide or CO ligand. For instance, treatment of **2** with one equiv. of KN(SiMe$_3$)$_2$ in THF at room temperature or −78 °C produced complicated mixtures that convert to **1** or its dimer, **1$_2$**, in less than a day. Interestingly, **1** is also produced when **2** is treated with two equivalents of Me$_3$NO in THF at room temperature or −78 °C along with a white ppt characterized as Me$_3$N·HBr. Attempts to remove the bromide ligands of **1**·HBr were performed in DCM with AgOTf, but this resulted in the formation of the triflate salt of the mono-protonated dimer (**1$_2$H-OTf**) and other intractable products. The ^{31}P NMR spectrum of **1$_2$H-OTf** contains two doublets at 73.22 and 63.52 ppm (J_{PP} = 43.56 Hz) (see ESI†). The same phosphorous signal was observed upon attempts to remove Br from **1**·HBr with Li[B(ArF$_5$)$_4$] and also treatment of **H-POP** with [Mn(CO)$_5$] OTf. Efforts to generate a 16-electron dicarbonyl complex from **1** were made by treating **1** with heat, photons and/or Me$_3$NO. As mentioned earlier, heating or irradiating **1** led to dimerization to **1$_2$**. Treatment of **1** with Me$_3$NO led to no reaction at room temperature and heating the mixture led to decomposition of the metal complex (the solution turned colorless from yellow and showed no CO peaks in FTIR).

Despite our current lack of success on producing 16 electron Mn(I) species with the **H-POP** platform, we also explored the efficacy of **1** as a hydrogenation catalyst under various conditions. During these investigations, we serendipitously discovered that **1** catalyzes the Tishchenko reaction with benzaldehyde in toluene (Scheme 4).[18] For instance, a 4 mol% loading of **1** in toluene with 0.4 M benzaldehyde and heating at 120 °C for 24 hours furnished benzyl benzoate with 26% conversion (TON ≈ 7, 24 h). Importantly, **1** does not react with benzyl alcohol in toluene, which serves as good evidence that the formation of benzyl benzoate proceeds through a Tishchenko reaction rather than one that involves dehydrogenation of alcohols or intermediate hemiacetals.[19–21]

We also tested other **H-POP** complexes (Table S1†) and interestingly found that **1$_2$** converts exactly twice as much reac-

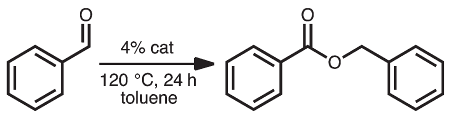

Scheme 4 Mn(I) catalyzed Tishchenko reaction.

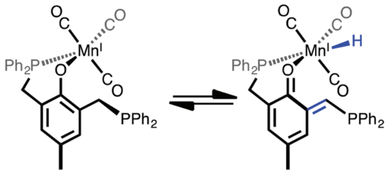

Scheme 5 Possible Mn(I) intermediates in the Tishchenko reaction.

tant than **1**. Considering the formation of $\mathbf{1_2}$ from **1** *via* heat or photolysis, we propose that a phosphine arm in **1** or $\mathbf{1_2}$ dissociates opening up a vacant site for the Mn(I)-phenoxide center to interact with benzaldehyde. Typical catalysts for the Tishchenko reaction are in fact metal alkoxides and therefore might provide some rationale as to why **1**, and not **2**, catalyzes the reaction. Specifically, the deprotonated phenoxide moiety in **1** serves to facilitate proton transfer or even a metal–ligand cooperative (MLC) step. The latter MLC reaction could result in a Mn(I)-hydrido intermediate with a dearomatized **POP** ligand in a quinone methide structure (Scheme 5).

In summary, we have explored the synthesis, coordination chemistry, and catalysis of a new pincer platform with Mn(I). A general finding is that the phenolic oxygen atom appears to weakly bind to Mn(I). Our conclusion on this matter is inferred by the small PhC–O–Mn angles in **1**, long or non-bonding Mn–O interactions, and our observation that the δ_{OH} and ν_{OH} do not shift much from the various complexes. This weak O–Mn interaction might also be responsible for the observed vast landscape of accessible species with the **H-POP** ligand, many of which were only observed as intermediates in ^{31}P NMR experiments. In addition, the studies herein are restricted to the cresol variant with only phenyl substituents on the phosphine arms. Undoubtedly, the tunability of phenols and phosphine ligands will furnish a wealth of new chemistry, which we are actively pursuing.

Conflicts of interest

There are no conflicts to declare.

Acknowledgements

Financial support was provided by the University at Buffalo start-up funds and an ACS Petroleum Research Fund (ACS-PRF-57861-DN13). This work was completed using the resources of the Chemistry Instrument Center (CIC), University at Buffalo, SUNY, Buffalo, NY; che-ic@buffalo.edu for sample inquiries.

References

1 C. Gunanathan and D. Milstein, *Chem. Rev.*, 2014, **114**, 12024–12087.
2 T. Zell and R. Langer, *ChemCatChem*, 2018, **10**, 1930–1940.
3 F. Kallmeier and R. Kempe, *Angew. Chem., Int. Ed.*, 2018, **57**, 46–60.
4 B. Maji and M. K. Barman, *Synthesis*, 2017, **49**, 3377–3393.
5 M. Garbe, K. Junge and M. Beller, *Eur. J. Org. Chem.*, 2017, 4344–4362.
6 A. Mukherjee, A. Nerush, G. Leitus, L. J. W. Shimon, Y. Ben-David, N. A. E. Jalapa and D. Milstein, *J. Am. Chem. Soc.*, 2016, **138**, 4298–4301.
7 S. Elangovan, C. Topf, S. Fischer, H. Jiao, A. Spannenberg, W. Baumann, R. Ludwig, K. Junge and M. Beller, *J. Am. Chem. Soc.*, 2016, **138**, 8809–8814.
8 G. M. Adams and A. S. Weller, *Coord. Chem. Rev.*, 2018, **355**, 150–172.
9 C. Zhu, N. Yukimura and M. Yamane, *Organometallics*, 2010, **29**(9), 2098–2103.
10 M. E. van der Boom, S.-Y. Liou, Y. Ben-David, L. J. W. Shimon and D. Milstein, *J. Am. Chem. Soc.*, 1998, **120**, 6531–6541.
11 A. Vigalok, B. Rybtchinski, Y. Gozin, T. S. Koblenz, Y. Ben-David, H. Rosenberg and D. Milstein, *J. Am. Chem. Soc.*, 2003, **125**, 15692–15693.
12 M. E. van der Boom, T. Zubkov, A. D. Shukla, B. Rybtchinski, L. J. W. Shimon, H. Rozenberg, Y. Ben-David and D. Milstein, *Angew. Chem., Int. Ed.*, 2004, **43**, 5961–5963.
13 K. Kellner, S. Rothe, E. M. Steyer and A. Tzschach, *Phosphorus Sulfur Relat. Elem.*, 1980, **8**(3), 269–273.
14 Đ. Škalamera, C. Bohne, S. Landgraf and N. Basarić, *J. Org. Chem.*, 2015, **80**(21), 10817–10828.
15 K. J. Kadassery, S. K. Dey, A. E. Friedman and D. C. Lacy, *Inorg. Chem.*, 2017, **56**, 8748–8751.
16 D. Himmelbauer, B. Stöger, L. F. Veiros and K. Kirchner, *Organometallics*, 2018, DOI: 10.1021/acs.organomet.8b00193.
17 S. J. A. Pope and G. Reid, *J. Chem. Soc., Dalton Trans.*, 1999, 1615–1621.
18 S. A. Morris and D. G. Gusev, *Angew. Chem., Int. Ed.*, 2017, **56**, 6228–6231.
19 N. Menashe and Y. Shvo, *Organometallics*, 1991, **10**, 3885–3891.
20 J. Zhang, G. Leitus, Y. Ben-David and D. Milstein, *J. Am. Chem. Soc.*, 2005, **127**, 10840–10841.
21 D. H. Nguyen, X. Trivelli, F. Capet, J.-F. Paul, F. Dumeignil and R. M. Gauvin, *ACS Catal.*, 2017, **7**, 2022–2032.